

# Morphology, crystallization and melting behaviors of isotactic polypropylene/high density polyethylene blend: effect of the addition of short carbon fiber

C. ZHANG

*Department of Organic and Polymeric Materials, Tokyo Institute of Technology, 2-12-1 Ookayama, Meguro-ku, Tokyo 152, Japan; College of Chemical Engineering, Zhejiang University of Technology, Hangzhou 310014, People's Republic of China*

X.-S. YI

*Department of Polymer Science and Engineering, Zhejiang University, Hangzhou 310027, People's Republic of China*

S. ASAI, M. SUMITA\*

*Department of Organic and Polymeric Materials, Tokyo Institute of Technology, 2-12-1 Ookayama, Meguro-ku, Tokyo 152, Japan  
E-mail: msumita@o.cc.titech.ac.jp*

The effect of vapor grown carbon fiber (VGCF) on the morphology, crystallization and melting behaviors of isotactic polypropylene (iPP)/high density polyethylene (HDPE) blend have been studied by means of Scanning Electron Microscopy (SEM) and Differential Scanning Calorimeter (DSC). It is found that the addition of VGCF results in a dramatic change in the morphology of iPP/HDPE blends. The crystallization peak temperature and melting point of iPP are not altered significantly by the blending. However, the degrees of crystallinity of iPP in the blends are reduced. Compared with the unfilled blends, the crystallization peak temperatures of iPP increase dramatically for the composites. The isothermal crystallization behavior of iPP is further investigated. The analysis of the crystallization half time shows that the crystallization rate of iPP is reduced by the presence of HDPE melt, and is enhanced by carbon fibers. For the unfilled blends in which iPP is the major component, the Avrami exponent closes to 3, independent of the HDPE content. However, for the composites, the Avrami exponent varies with the composition in a rather complex manner. An explanation based on heterogeneous and homogeneous nucleation is supposed. The sharp changes in the crystallization and melting behaviors for the composites containing 30–35wt% HDPE correspond to the sudden change in the morphology of the two phases. It is supported by the observation of SEM and the electrical measurement. © 2000 Kluwer Academic Publishers

## 1. Introduction

The technique of blending two polymers for obtaining a balanced combination of properties has been recognized as a cost-effective method to tailor-make materials to meet specific end-use requirements [1–6]. The ultimate properties of the blends consisting of two crystallizable polymers are determined partly by the crystalline morphology of the blends, which in turn depends on the relative rates of nucleation and crystal growth of the component polymers. The constituent polymers can either crystallize at the same time or separately in sequential manner, leading to different morphologies and hence different properties. Thus, in a blend contain-

ing two crystalline polymers, the physical properties of the blends may be altered not only by the composition but also by changing their relative crystallization behavior. Depending upon the difference in the melting points of the component polymers, the crystallization conditions would change. For example, if the difference in the melting points is small, both the polymers might crystallize over the same temperature range. On the other hand, if the melting point difference is significant, then one of the components would crystallize in the presence of the melt of the other component. Whereas the second component in this case would crystallize in the presence of the solid phase of the first

\* Author to whom all correspondence should be addressed.

component. The presence of the second fluid or solid phase would influence the relative rate of crystallization and the degree of crystallinity, thereby modify the morphology.

Martuscelli has reviewed the effect of composition and crystallization condition on the morphology and crystallization behavior of polymer blends [7]. He has presented the results in terms of various parameters such as radial growth rate, overall rate of crystallization, equilibrium melting point, lamella thickness and long period. In the case of compatible crystalline/amorphous blends, a decrease in the radial growth rate and a depression in melting point was observed with increasing content of noncrystalline component. In the case of crystalline/crystalline blends, a decrease in the radial growth rate, long period and lamella thickness was observed. Santana and Muller have studied the crystallization behavior of isotactic polypropylene (iPP) blended with atactic polystyrene (PS) [8]. It has been found that the nucleation mechanism of iPP in immiscible iPP/PS blends can be strongly influenced by the morphology of the blends. If iPP component is finely dispersed in the matrix of the amorphous PS component, the nucleation mechanism changes from preferentially heterogeneous to preferentially homogeneous as the size of the dispersed iPP domain decreases below a critical value. In a study of blends of polypropylene with poly-1-butene, Siegmann reported that the crystallization process of two components was significantly affected, resulting in a lower degree of crystallinity, depression in melting point and a change in morphology from spherulitic to branched crystallites [9]. The crystallization behavior of iPP blended with ethylene-propylene copolymers (EPR) was studied by Greco [10]. The results showed that the overall crystallinity of iPP decreased for the blends with respect to pure iPP.

The properties of the blends containing two crystallizable components depend strongly on their crystallinity, crystalline morphology and degree of dispersion [11–18]. The presence of dispersed particles might cause large changes not only in the morphology of the continuous phase, but also on the overall kinetics of crystallization and spherulite growth rate. The blends of iPP with low or high density polyethylene (LDPE, HDPE) have been investigated by several authors [19–23]. It has been found that iPP is immiscible with polyethylene, and the blend forms a heterogeneous two-phase system. PE inclusions in iPP matrix constitute geometrical obstacles to spherulitic growth and cause large changes in their morphology, but they have very little effect on the growth rate [24]. On the other hand, large changes have been reported in the overall kinetics of crystallization and in the spherulite nucleation in blends compared to pure polypropylene [25]. Gupta *et al.* have reported an enhancement in nucleation, reduction in size of crystallites and a lower degree of crystallinity in the polypropylene blended with high density polyethylene [26].

For a crystalline polymer filled with fibers, the fibers have the potential to modify dramatically the crystal-

lization characteristics of the polymer matrix. Recently, many efforts have been made to characterize the effect of filler on the crystallization of a variety of thermoplastic polymers [27–33]. Experimental evidence confirms that fibers can influence the crystallization kinetics and morphology of the matrix. The fiber surface may act as a nucleating agent during processing a carbon fiber filled polymer. In this case, the morphology of the polymer is considerably altered in the vicinity of the nucleating fiber surface. The subtle nature of the interlayer region between polymer and fiber, or the interphase, is crucial in determining the properties of polymer composites. So, the modification of crystalline morphology promoted by fibers is of great interest and it has become the central goal of many studies [34].

Although the morphology, crystallization and melting behaviors for either binary polymer blends or one crystalline polymer containing filler systems have been extensively studied. But there are few reports in the literature dealing with systematic studies of crystallization for the polymer blends containing fillers. The main reason may be due to the difficulty of the investigation resulting from the complexity of this field. For industrial purposes, however, polymer blends are usually used in the presence of fillers. Therefore, a scientific study of the influence of the filler on morphology, crystallization and melting behavior of the component polymers in the blend is essential to the understanding of how to optimize processing conditions and properties. In our previous papers [35, 36], we have reported that vapor-grown carbon fiber (VGCF) is selectively located in the HDPE phase for VGCF filled iPP/HDPE and HDPE/PMMA blends systems. The preferential accumulation of fillers in the HDPE phase results in the formation of conductive network in this phase at very low total filler content, and enhances the conductivity of the composites. The electrical properties depended on both the dispersion state of the fillers and the morphology of the blends. It can be expected that the dispersion of carbon fibers may be affected by the crystallization behavior of the components during the polymers crystallized from melt, on the other hand, carbon fibers can influence the crystallization kinetics and morphology of the matrix. In the present work, the effects of carbon fibers and HDPE on the morphology, crystallization and melting behaviors of iPP have been studied.

## 2. Experimental

### 2.1. Materials and preparations

High density polyethylene (HDPE) (E891(C), from Nihon Sekiyu Kagaku Co.) and isotactic polypropylene (iPP) (FA110, from Showa Denko Co.) were used as matrices. Vapor grown carbon fiber (VGCF) (average length 10  $\mu\text{m}$ , average diameter 0.2  $\mu\text{m}$ , from Showa Denko Co.) was used as a filler. The polymers were firstly mixed on a two-roll mill at the temperature of 190°C for 5 min, followed by adding the filler into the mixture and mixing for 10 min. Prior to the mixing, the polymers were dried at 80°C for 24 h, and the filler was

dried at 130 °C for 3 h under vacuum. The samples were molten at 190 °C for 10 min and compressed under the pressure of 18 MPa for 15 min, followed by quenching into water to obtain the films with the thickness of 0.5 mm.

## 2.2. Observation of scanning electron microscopy (SEM)

The samples were heated at a rate of 10 °C/min up to 200 °C, kept for 5 min, cooled at 5 °C/min to 160 °C, then cooled at 0.5 °C/min to 80 °C using a hot stage

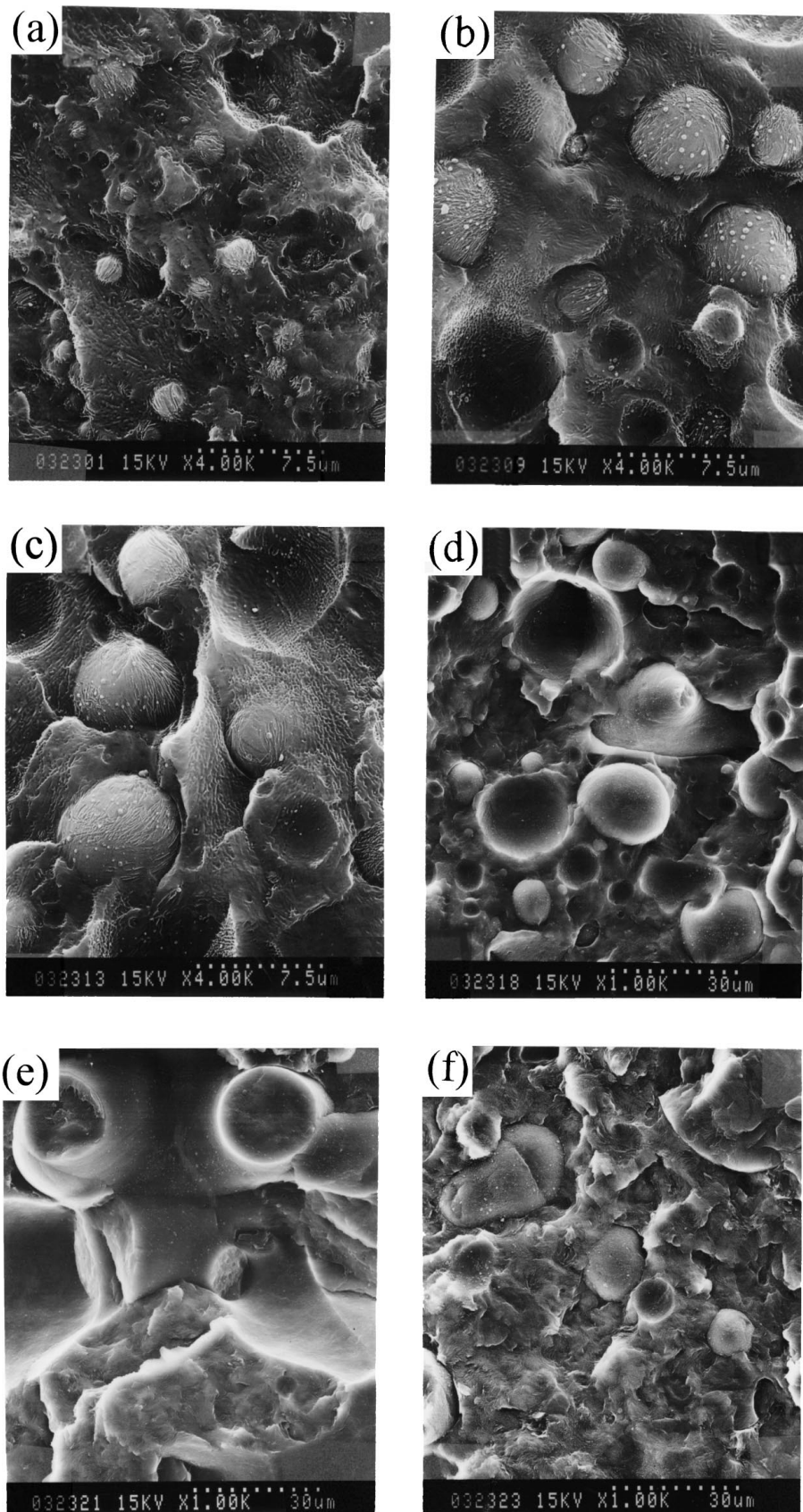


Figure 1 SEM micrographs of HDPE/iPP (a) 20/80, (b) 30/70, (c) 35/65, (d) 40/60, (e) 50/50 and (f) 70/30 blends. (Page 8, Line 10).

under the nitrogen gas atmosphere, finally quenched into water. The surface of the samples, which was fractured in liquid nitrogen, etched with an Eiko IB-3 and coated with Pt-Pd, was observed by a FE S800 Scanning Electron Microscopy.

### 2.3. Differential scanning calorimeter (DSC) measurement

The DSC measurement for the non-isothermal crystallization was carried out using a Shimadzu DSC-50 Differential Scanning Calorimeter under the nitrogen gas atmosphere at a flow rate of 30 ml/min. The samples were cut into the small pieces, and were weighed in aluminum pans (about 8 mg). The  $\text{Al}_2\text{O}_3$  powder was used as the reference. The samples were heated at a rate of  $10^\circ\text{C}/\text{min}$  up to  $200^\circ\text{C}$ , kept for 5 min, cooled at  $5^\circ\text{C}/\text{min}$  to  $160^\circ\text{C}$ , and then cooled at  $0.5^\circ\text{C}/\text{min}$  to  $80^\circ\text{C}$ , finally reheated at  $10^\circ\text{C}/\text{min}$  to  $200^\circ\text{C}$ . The melting parameters of the samples were determined from the reheating scans. The heat of crystallization was calculated from the cooling scans.

A SEIKO module 2000 Differential Scanning Calorimeter was utilized to study the isothermal crystallization behavior. A nitrogen purge gas was provided throughout the measurement. The samples were heated to  $200^\circ\text{C}$  for 5 min to achieve complete melting and destruction of residual iPP nuclei, then rapidly quenched to the designated crystallization temperature. Crystallization from the melt was only possible at the temperature of  $126.5^\circ\text{C}$  for the blends and  $132.5^\circ\text{C}$  for the composites, respectively. Two factors were considered to choose the crystallization temperature. One consideration is the crystallization of iPP can complete within an acceptable time at this temperature for all the samples. Another is the crystallization temperature can be achieved prior to the initiation of crystallization. Because the cooling rates of the DSC instrument used were not sufficiently fast, the latter factor was more critical for the samples filled with short carbon fibers. The total crystallization time was determined as the time required from the onset of the peak till a steady baseline was obtained.

## 3. Results and discussion

### 3.1. Morphology after non-isothermal crystallization

It is well known that iPP/HDPE blend is a heterogeneous two-phase system, the components of which crystallize separately into discrete phases. In order to investigate the effect of VGCF filler on the morphology of iPP/HDPE blends, the SEM micrographs of iPP/HDPE unfilled blends after non-isothermal crystallization are carried out to give a valid comparison to the blends filled with VGCF. The dispersed phase content has a significant effect on the domain size [37, 38], while the type of stress field is more significant for the domain shape [39]. The combined effects of droplet deformation, orientation, and coalescence determine the structure development during processing. As shown in Fig. 1, at lower HDPE contents, where the spherical domains of

HDPE are dispersed in the iPP matrix, and domain size of HDPE increases with increasing HDPE content. The explanation is that an increase in the HDPE content increases the number of dispersed droplets, which enhances the collision-coalescence phenomenon among HDPE droplets, and leads to a larger dispersed domain size [40]. As a consequence, the large domains are no longer stable, and then can be deformed into irregular shape (Fig. 1d), finally develop to a continuous structure (Fig. 1e). Interestingly, a comparison of dispersed domain size for the blends containing 30 wt % HDPE and 30 wt % iPP (Fig. 1b and f) shows that the average size of the HDPE domains dispersed in iPP,  $10\text{--}20\ \mu\text{m}$ , are larger than that of the iPP domains dispersed in HDPE,  $5\ \mu\text{m}$ . This asymmetry in domain size with the composition has been observed in other blend systems as well, such as PE/PS, PE/PC [41] and PP/PC [37].

The SEM micrographs of iPP/HDPE blends filled with 1.5 phr VGCF are shown in Fig. 2. We can find clearly that carbon fibers are preferentially located in the HDPE phase. As discussed in our previous paper [35], this heterogeneous distribution of carbon fibers between the two phases is due to the difference in affinity of the filler to each component of the polymer blend. The driving force for the migration of VGCF between the components of the blends is the interfacial free energy difference when VGCF is surrounded by iPP melt and by HDPE melt, respectively [42–44]. Compared with the unfilled blends, the HDPE domains become more irregular for VGCF filled iPP/HDPE blends (Fig. 2). An interesting point should be noted that the addition of VGCF results in the formation of a co-continuous structure of the HDPE phase in the blends at a lower HDPE content. When the HDPE content reaches to 30–35wt%, the continuous structure of the HDPE phase starts to be formed (Fig. 2b and c). However, at the same HDPE content, the HDPE domains are dispersed in the iPP matrix for the unfilled blends (Fig. 1b and c). This indicates that the addition of VGCF can affect the morphology of the blends. The explanation is that VGCF more likely increases the HDPE melt viscosity and perturbs the kinetics of the phase coalescence during the mixing and molding process [36, 45].

### 3.2. Non-isothermal crystallization

Generally, the crystallization behavior of polymer is studied by the isothermal method. However, the study of the non-isothermal crystallization of polymer is of great technological significance since most practical processing techniques proceed under non-isothermal conditions. Fig. 3 shows the effect of cooling rate on the non-isothermal crystallization of iPP50/HDPE50 blends filled with 1.5 phr VGCF from the melt. It is found that all the samples exhibit two distinct crystallization peaks at low cooling rates ( $0.5$  and  $1^\circ\text{C}/\text{min}$ ). But when cooling rate is high, the overlapping of crystallization peaks appears on the thermograms. It can also be seen that with increasing cooling rate, both the crystallization peaks of iPP and HDPE are shifted to lower temperatures. However, the shift of the former is faster than that of the later. So the overlapping of two crystallization peaks occurs.

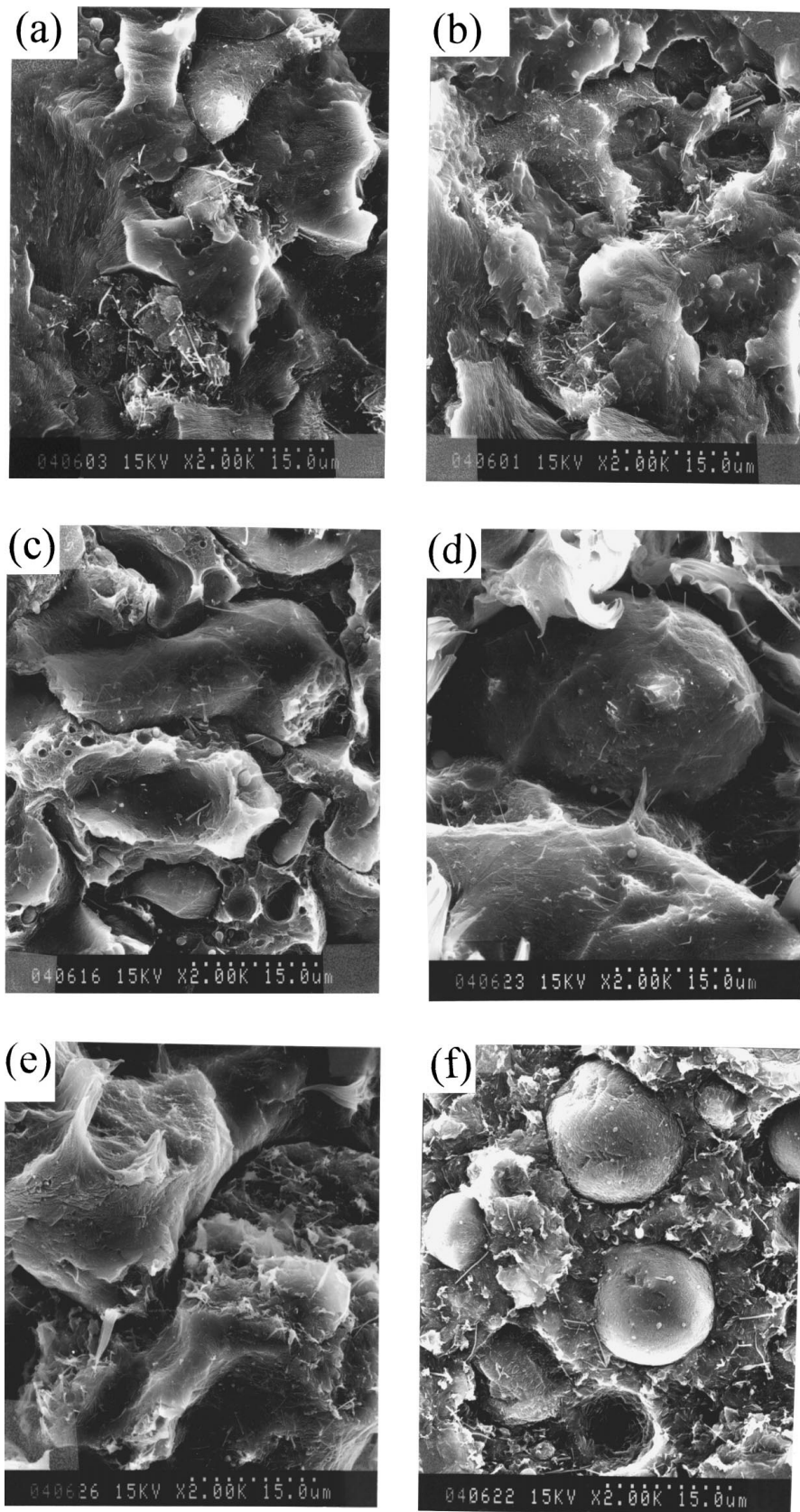


Figure 2 SEM micrographs of 1.5 phr VGCF filled HDPE/iPP (a) 20/80, (b) 30/70, (c) 35/65, (d) 40/60, (e) 50/50, and (f) 70/30 blends. (Page 8, Line 22).

Further measurements of the non-isothermal crystallization for the unfilled blends and the composites containing 1.5 phr VGCF are carried out at a cooling rate of  $0.5^{\circ}\text{C}/\text{min}$ . The DSC scans are shown in Fig. 4. It is clear that the crystallization exothermic peaks of iPP

are not altered significantly by the blending (Fig. 5). However, the heats of crystallization ( $H_c$ ) of iPP for unfilled blends are lower than that of virgin polymer (Fig. 6), indicating that the degree of crystallinity is reduced by the blending. With increasing HDPE content,

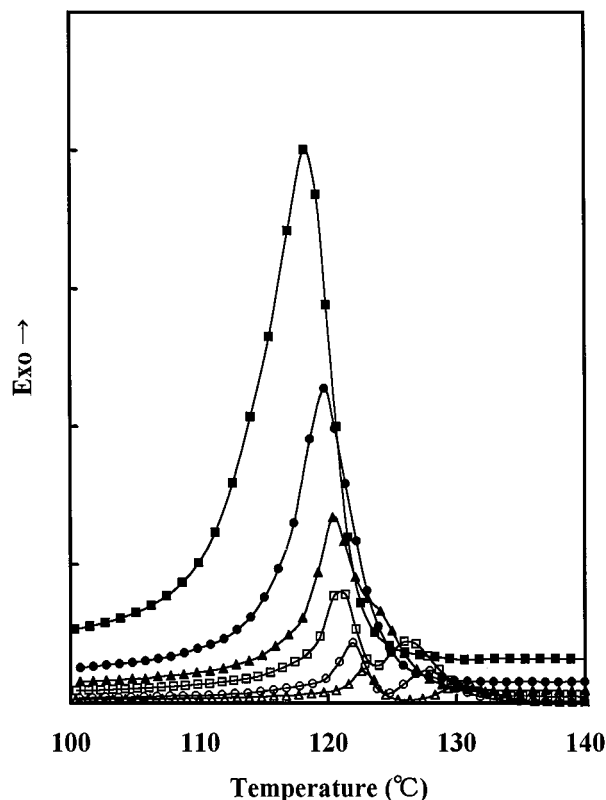


Figure 3 DSC crystallization exotherms of 1.5 phr VGCF filled iPP/HDPE (50/50) blends at different cooling rates: (■) 10°C/min, (●) 5°C/min, (▲) 3°C/min, (□) 2°C/min, (○) 1°C/min and (△) 0.5°C/min. (Page 9, Line 18).

the  $H_c$  of iPP decreases, except for iPP65/HDPE35 blends, where a sharp increase in the  $H_c$  of iPP is observed.

Returning to Fig. 4, it is observed that the crystallization peak temperatures ( $T_c$ ) of iPP increase considerably, and vary with HDPE content in a rather complex manner due to the addition of VGCF. For VGCF filled virgin iPP, an increase in  $T_c$  can be attributed to a heterogeneous nucleation provided by carbon fibers. But for VGCF filled iPP/HDPE blends, two opposite tendencies can be proposed. One is that the selective location of carbon fibers in the HDPE melt leads to a decrease in the number of heterogeneous nuclei in the iPP melt, thus reduces the crystallization of iPP. As the HDPE content in the blend increases, the probability of the migration of carbon fibers from iPP to HDPE melt will increase. This will induce a decrease in the  $T_c$  of iPP. On the other hand, as can be seen in Fig. 2, the average length of carbon fiber, 10  $\mu\text{m}$ , is comparable to the domain size of HDPE, some carbon fibers near the boundaries between the HDPE and iPP melts penetrate into the iPP phase. These carbon fibers which are surrounded by the HDPE melt can also act as a nucleating agent for iPP, and appear to have a more active nucleating effect than that of pure HDPE melt, considering the  $T_c$ s of iPP for unfilled blends increase only slightly due to the blending. The similar effect was reported by Hammer and Maurter for BaSO<sub>4</sub> filled PP/PP-g-MAH/PS system [46]. For PP homopolymer, PP/PP-g-MAH blend, BaSO<sub>4</sub> filled PP and PP/PS blend, the DSC crystallization peak temperature of PP is near 111°C. However, when PP-g-MAH

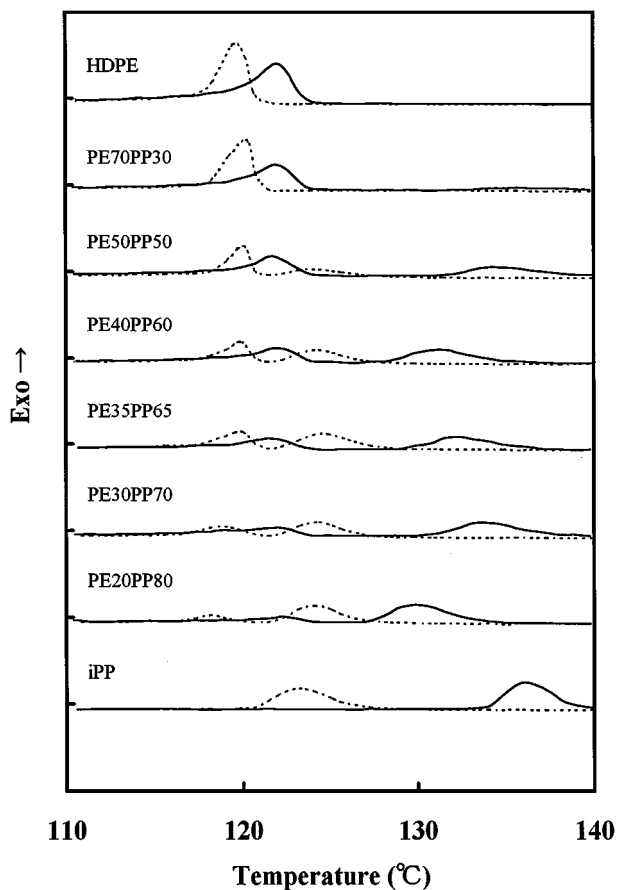


Figure 4 DSC crystallization exotherms of unfilled (broken lines) and 1.5 phr VGCF filled (solid lines) iPP/HDPE blends at a cooling rate of 0.5°C/min. (Page 10, Line 3).

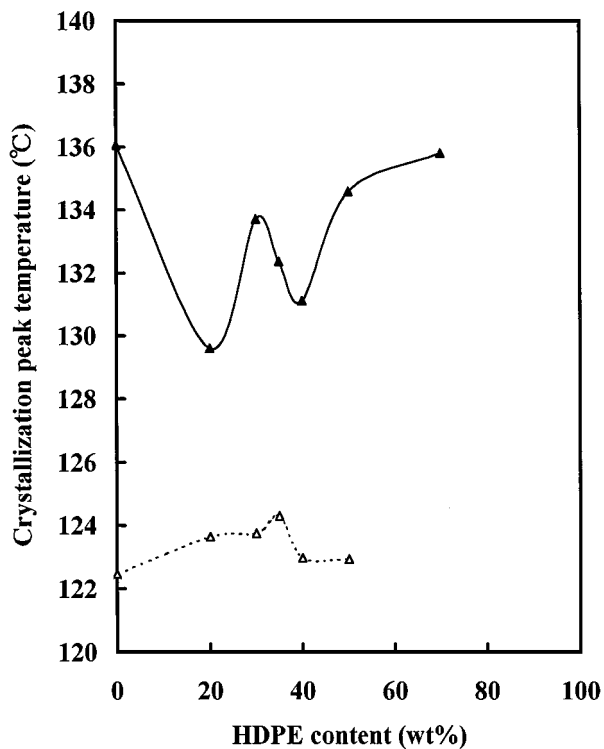


Figure 5 Dependence of crystallization peak temperatures of iPP on HDPE content for (△) unfilled and (▲) 1.5 phr VGCF filled iPP/HDPE blends. (Page 10, Line 4).

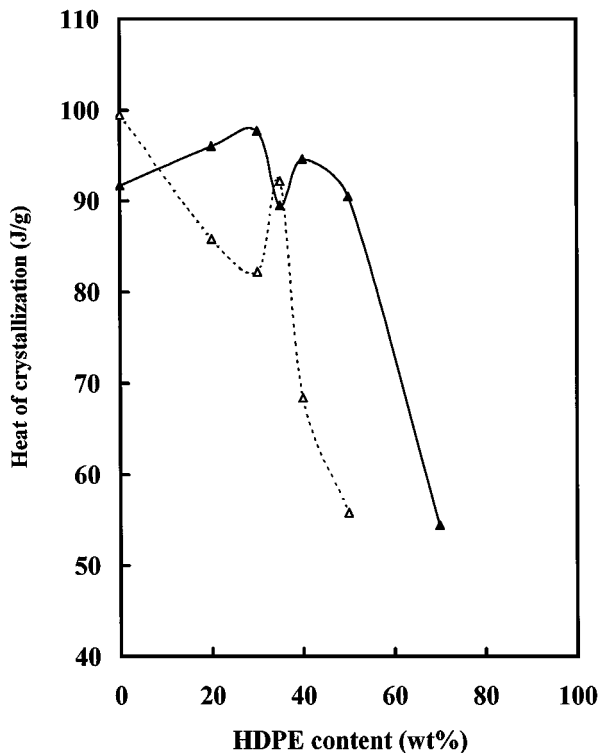


Figure 6 Dependence of heat of crystallization of iPP on HDPE content for ( $\Delta$ ) unfilled and ( $\blacktriangle$ ) 1.5 phr VGCF filled iPP/HDPE blends. (Page 10, Line 5).

was added to BaSO<sub>4</sub> filled PP/PS blend system, the  $T_c$  of iPP jumped to 123°C. In their case, BaSO<sub>4</sub> is selectively located in the PP phase, and surrounded by PP-g-MAH. The increase in the  $T_c$  of iPP was supposed to be due to the effect of the specific adhesion of PP-g-MAH to the filler surface, which probably results in a lower loss of entropy upon crystallization. The migration of heterogeneous nuclei from iPP to HDPE melts for iPP/HDPE system was also observed by Bartzczak *et al.* [44]. According to the authors' explanation, the HDPE crystals growing near the surface of the nucleating agents (magnesium sulphate and sodium bezoate) could act as nucleating agents for iPP near the boundaries of HDPE and iPP melt, and enhanced the nucleation of iPP. So for VGCF filled iPP/HDPE blends, the overall crystallization behavior of iPP is a combined effect of above two tendencies. In this case, the interface between the HDPE and iPP phases may play an important role in the crystallization process. As the HDPE content in the blend increases, the HDPE domains are elongated from spherical into strip shape, resulting in an increase in the interface area between the HDPE and iPP phases, as well as the probability of the contacts of iPP melt with the carbon fibers which are surrounded by the HDPE melt. This will accelerate the crystallization process of iPP. It can be imaged that, when the HDPE phase develops from dispersed domains to a continuous structure, a sudden change in surface area can be expected. As a result, a peak of  $T_c$  occurs for the composites containing 30–35 wt% HDPE, which corresponds to the sudden change in the morphology of the blends, where a continuous structure of HDPE phase starts to be formed. The heats of crystallization of iPP are comparable for all the compositions except

for the composite containing 70 wt% HDPE, where a dramatic decrease in the heat of crystallization is observed (Fig. 5), indicating the crystal growth of iPP is impeded by the HDPE melt when HDPE is the major phase in the blend.

### 3.3. Melting behavior after non-isothermal crystallization

The DSC reheating scans of the blends and the composites were used to determine two parameters signifying the melting behavior of iPP. The melting parameters include melting point ( $T_m$ ) and heat of fusion ( $H_f$ ) determined from the reheating scans after non-isothermal crystallization. It should be noted that the first heating scans of the as-prepared samples cannot be compared in view of the different and uncontrolled quench conditions encountered by the different samples. The DSC scans of the blends and the composites at a reheating rate of 10°C/min are shown in Fig. 7. Both the unfilled and 1.5 phr VGCF filled blends exhibit two distinct melting peaks.

The melting points ( $T_m$ ) of iPP for the unfilled blends are independent of the composition, except for iPP30/HDPE70 blend, where a slight decrease in  $T_m$  is observed. However, for the filled blends, the  $T_m$ s of iPP are considerably higher than those for the unfilled blends, and vary with the composition (Fig. 8). Since the  $T_m$  depends on the crystalline size, which in turn depends on the number of primary nuclei, the variation

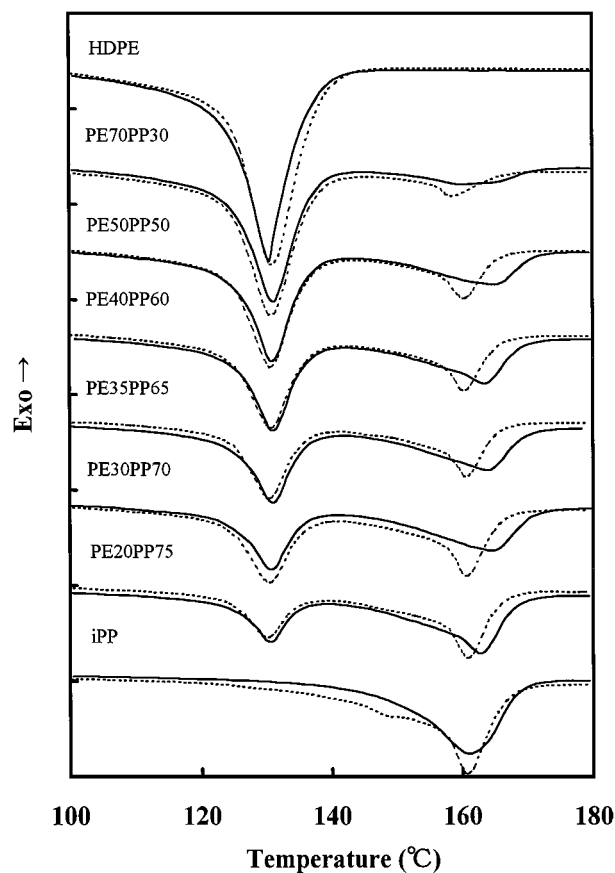


Figure 7 DSC reheating curves of unfilled (broken lines) and 1.5 phr VGCF filled (solid lines) HDPE/iPP blends after non-isothermal crystallization (Page 12, Line 7).

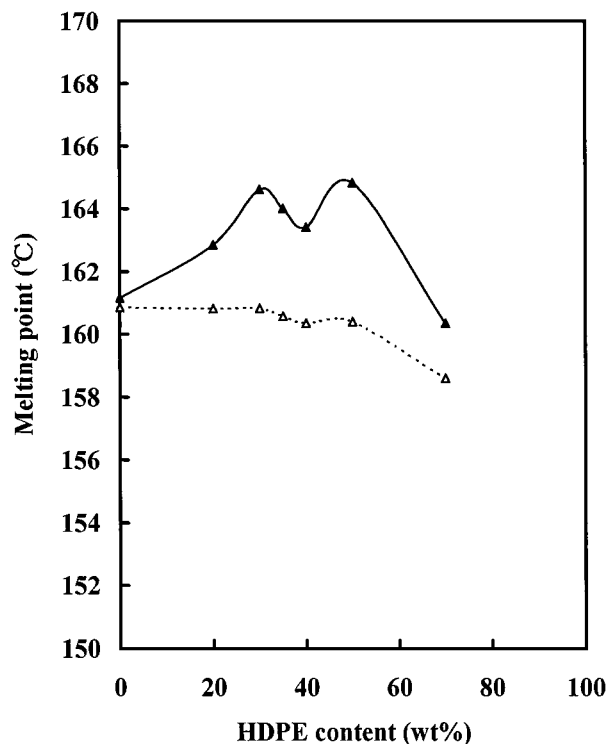


Figure 8 Dependence of melting point of iPP on HDPE content for ( $\Delta$ ) unfilled and ( $\blacktriangle$ ) 1.5 phr VGCF filled iPP/HDPE blends. (Page 12, Line 12).

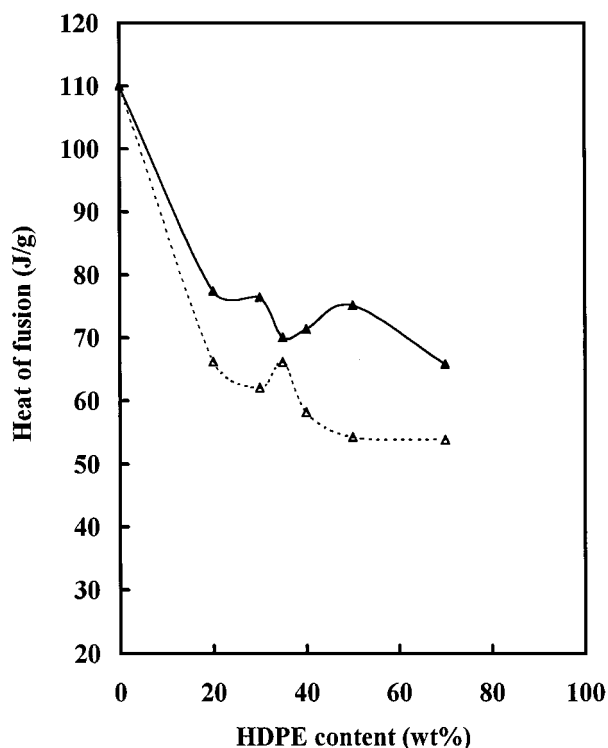


Figure 9 Dependence of heat of fusion of iPP on HDPE content for ( $\Delta$ ) unfilled and ( $\blacktriangle$ ) 1.5 phr VGCF filled iPP/HDPE blends. (Page 12, Line 14).

of  $T_m$  may reflect the change in the number of heterogeneous nuclei. Fig. 9 shows the variations of heats of fusion of iPP for the unfilled blends and the composites. The degrees of crystallinity of iPP for both the unfilled and filled blends are considerably lower than that of the virgin polymer, as indicated by the heats of fusion. The

slight increase of crystallinity of iPP for the composites can be explained on the basis of the heterogeneous nucleation provided by the VGCF which are surrounded by the HDPE melt.

### 3.4. Isothermal crystallization behavior

The crystallization peak temperature of iPP is much higher than that of HDPE. Therefore, iPP crystallization will occur in the presence of the HDPE melt. The effects of the HDPE melt and the filler on the isothermal crystallization behavior of iPP were further investigated.

Two typical isothermal crystallization exotherms for the unfilled and VGCF filled iPP50/HDPE50 samples are shown in Fig. 10. The heat flow to or from the DSC cell is measured as a function of time at a constant crystallization temperature. The crystallization process is exothermic, and the total area under the exothermic crystallization curve is the heat of crystallization  $\Delta H_c$ . Because the crystallization process of iPP is accelerated by the filling, a higher crystallization temperature was chosen for the composites.

The relative amount of crystallinity,  $X_t$  is defined as the ratio of the weight fraction crystallinity at time  $t$  to the ultimate weight fraction crystallinity. It can be obtained by:

$$X_t = \frac{\int_0^t \left(\frac{dH}{dt}\right) dt}{\int_0^\infty \left(\frac{dH}{dt}\right) dt} \quad (1)$$

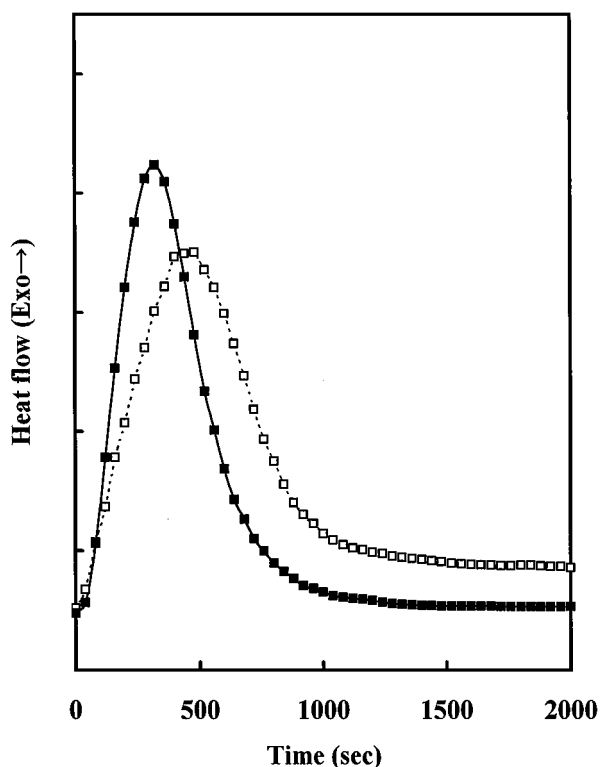


Figure 10 Typical crystallization isotherms of iPP for iPP50/HDPE50 blends ( $\square$ ) unfilled crystallized at 126.5°C and ( $\blacksquare$ ) filled with 1.5 phr VGCF crystallized at 132.5°C. (Page 13, Line 2).



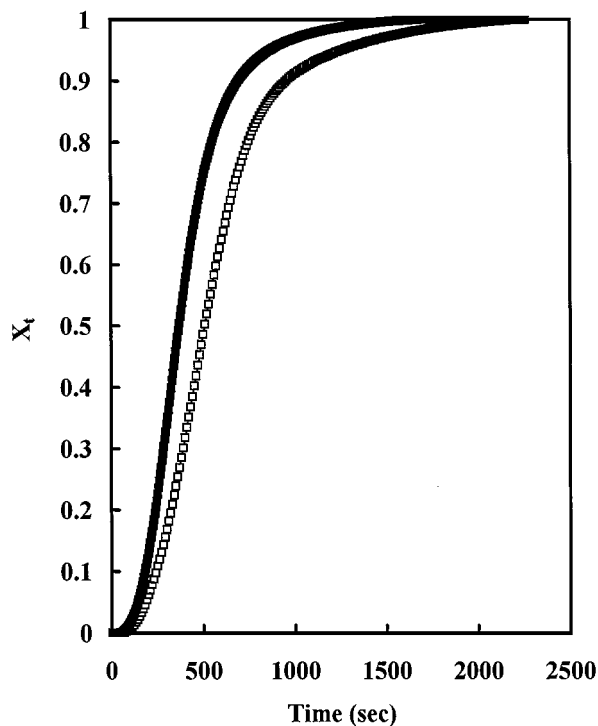


Figure 11 Typical relative crystallinity of iPP as a function of time for iPP50/HDPE50 blends (□) unfilled crystallized at 126.5°C and (■) filled with 1.5 phr VGCF crystallized at 132.5°C. (Page 13, Line 14).

where  $dH/dt$  is the rate of heat evolution as a function of time. This is achieved by determining the area under the isothermal crystallization curve point by point, and taking the ratio of the areas at each time interval to total area.

Fig. 11 illustrates the relative amount of crystallinity ( $X_t$ ) plotted as a function of time for the unfilled and 1.5 phr VGCF filled iPP50/HDPE50 blends. It can be seen that the crystallization rate for the composites is faster than that for the blends even at a higher crystallization temperature. An important quantitative parameter used to describe crystallization kinetics is the crystallization half time,  $t_{1/2}$ , which is defined as the time at which the normalized crystalline content reaches to 0.5. To understand how the overall crystallization rate of iPP is affected by the HDPE content and the filler, the crystallization half times of iPP are compared. Fig. 12 shows the dependence of the crystallization half time of iPP on the HDPE content for the unfilled blends and the composites. It is observed that for the unfilled blends, the crystallization half times of iPP are longer than that of virgin iPP, and increase with increasing HDPE content for those compositions wherein the iPP phase forms a continuous structure. Thus, in this case, the crystallization rate is reduced by the presence of the HDPE melt. Whereas for the blend containing 70 wt % HDPE, in which iPP domains are dispersed in the molten HDPE phase, the crystallization rate of iPP is enhanced.

Unlike the unfilled blends, the crystallization half times of iPP for the blends filled with 1.5 phr VGCF vary with the composition in a rather complex manner. As discussed above, this can be attributed to the two opposite tendencies. As expected, a sharp decrease in  $t_{1/2}$  is observed for the composites containing 30–35wt% HDPE, where the co-continuous structure of two phases

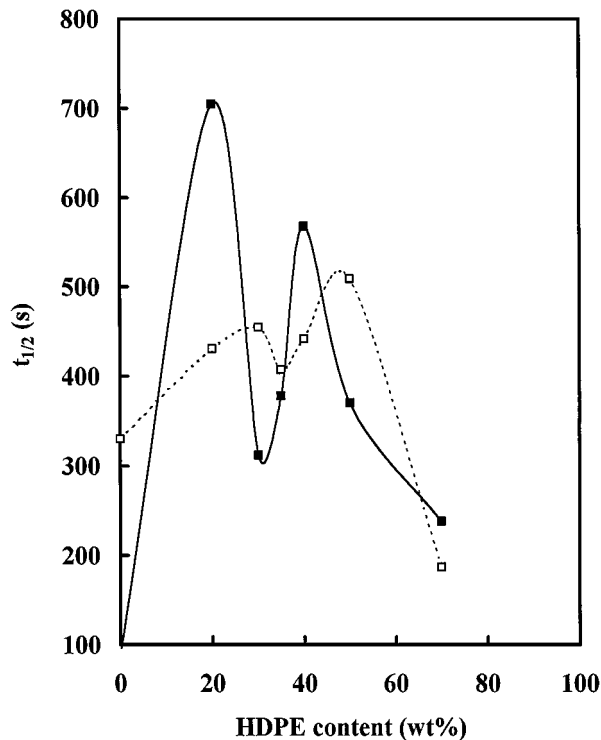


Figure 12 Dependence of crystallization half time of iPP on HDPE content for iPP/HDPE blends (□) unfilled crystallized at 126.5°C and (■) filled with 1.5 phr VGCF crystallized at 132.5°C. (Page 13, Line 21).

starts to be formed, indicating that the crystallization rate of iPP is enhanced in this case. However, for the unfilled blends, the bottom position is shifted to a higher HDPE content, i.e., 35–40wt%. Therefore, the isothermal crystallization behavior of iPP also depends on the morphology of the blend. It is suggested that the morphology of the blend can be characterized by the study of crystallization.

The Avrami equation [47] is used to model the primary crystallization kinetics. The general form of the Avrami equation is:

$$1 - X_t = \exp(-Kt^n) \quad (2)$$

where  $X_t$  is the relative amount of crystallinity at time  $t$ ,  $K$  is the crystallization rate constant depending on nucleation and growth rates, and  $n$  is the Avrami exponent, which is related to the type of nucleation mechanism and the geometry of crystal growth. The parameters in equation (2) can be determined by twice taking the logarithm of this equation,

$$\log[-\ln(1 - X_t)] = \log K + n \log t \quad (3)$$

Consequently, a plot of  $\log[-\ln(1 - X_t)]$  vs.  $\log t$  permits the determination of  $\log K$  from the intercept, and  $n$  from the slope of the straight line. Two typical Avrami plots for unfilled and 1.5 phr VGCF filled HDPE50/iPP50 samples are shown in Fig. 13.

From the Avrami plots for all the unfilled blends and the composite samples, both the primary crystallization and the secondary crystallization periods can be observed. The Avrami exponent  $n$  and Avrami rate constant  $K$  obtained from the Avrami plots are summarized in Table I. For the unfilled blends in which

TABLE I Avrami exponents and Avrami rate constants obtained from Avrami plots of iPP for unfilled and 1.5 phr VGCF filled iPP/HDPE blends

HDPE Content	Without VGCF <sup>a</sup>		With 1.5 phr VGCF <sup>b</sup>	
	<i>n</i>	log( <i>K</i> )	<i>n</i>	log( <i>K</i> )
0	3.01	-7.40	2.22	-4.56
20	2.98	-8.01	4.06	-11.43
30	3.19	-8.62	3.03	-7.67
35	3.01	-8.00	3.45	-8.90
40	2.99	-8.07	3.34	-9.28
50	2.70	-7.45	2.89	-7.56
70	1.46	-3.31	2.99	-7.09

<sup>a</sup>crystallized at 126.5°C.

<sup>b</sup>crystallized at 132.5°C.

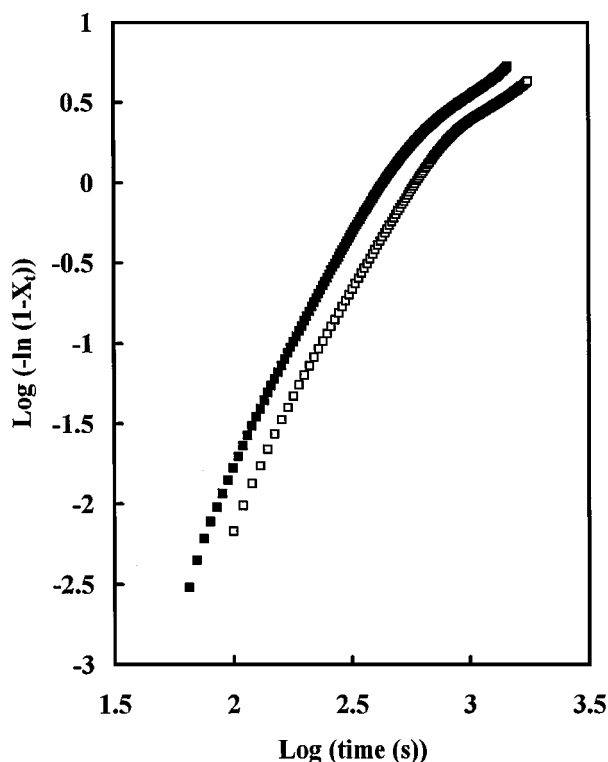


Figure 13 Typical Avrami plots of iPP for iPP/HDPE blends (□) unfilled crystallized at 126.5°C and (■) filled with 1.5 phr VGCF crystallized at 132.5°C. (Page 14, Line 23).

iPP is the major component, *n* closes to 3, independent of HDPE content, implying a growth of three-dimensional spherulitic superstructures following heterogeneous nucleation. But for the blend containing 70wt% HDPE, *n* decreases to 1.46. It can be explained that, because iPP crystallizes in the presence of molten HDPE, the HDPE melt will retard the crystal growth of iPP by restricting the diffusion of iPP chain to the nuclei. The retarding influence on the crystal growth will be more prominent for the blends wherein HDPE is a major phase. A value of 1.46 for Avrami exponent could imply the incomplete development of the crystallites or a growth of two-dimensional crystallites (discs). However, for the composites, *n* varies with the HDPE content in a rather complex manner. For virgin polymer filled with 1.5 phr VGCF, *n* is 2.2, indicating heterogeneous nucleation and two-dimensional crystal growth.

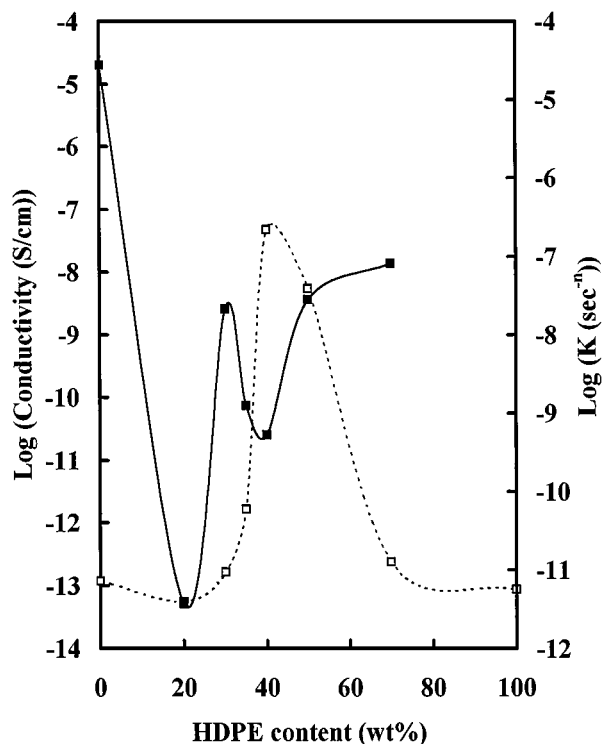


Figure 14 Dependence of (Δ) electrical conductivity and (■) Avrami rate constant on HDPE content for iPP/HDPE blends filled with 1.5 phr VGCF. (Page 16, Line 2).

The iPP crystallites besides carbon fibers can act as heterogeneous nuclei, thereby accelerating the crystallization process. But for the blends filled with 1.5 phr VGCF, since carbon fibers are selectively located in the HDPE phase, the nucleation mechanism is different from that for virgin polymer composite. For the composite containing 20 wt % HDPE, due to the disappearance of VGCF heterogeneous nuclei, *n* is 4.1, indicating a homogeneous nucleation and three-dimensional crystal growth. However, as discussed above, carbon fibers surrounded by HDPE near the boundaries of HDPE and iPP melts can also act as a nucleating agent for iPP. When the co-continuous structure of the two phases starts to be formed, the nucleation effect of later factor on the crystallization of iPP becomes more prominent. The heterogeneous nucleation of iPP will be enhanced. So the overall crystallization is the combined effects of heterogeneous and homogeneous nucleation.

In a previous paper [35], we reported that the electrical properties of VGCF filled iPP/HDPE blends also depended on the morphology of the blends. Comparing the variation of conductivity with that of Avrami rate constant for iPP/HDPE blends filled with 1.5 phr VGCF as a function of HDPE content (Fig. 14), it can be observed that both the conductivity and Avrami rate constant change sharply for the composites containing 30–35wt% HDPE. According to the discussions in our published paper and the previous section, these dramatic changes in conductivity and Avrami rate constant should correspond to the formation of the co-continuous structure in the composites. This suggests that both the electrical measurement and crystallization investigation can also be used to characterize the morphology of polymer blends.

#### 4. Conclusions

It is concluded that the morphology of iPP/HDPE blends is strongly affected by the addition of short carbon fiber. The addition of VGCF results in the formation of co-continuous structure of the two phases at a lower HDPE content. The crystallization and melting behaviors of iPP are related to the morphology of iPP/HDPE blends. The crystallization peak temperature and melting point of iPP are not altered significantly by the blending. However, the degrees of crystallinity of iPP in the blends are reduced. Compared with the unfilled blends, the crystallization peak temperatures and melting point of iPP increase dramatically for the composite. But there is only a little influence of the filling on the degrees of crystallinity of iPP. The variation of crystallization peak temperatures of iPP corresponds to the change in the morphology of the composites.

The investigation of isothermal crystallization behavior of iPP shows that the crystallization rate is reduced by the presence of HDPE melt, and is enhanced by carbon fibers. For the unfilled blends in which iPP is the major component, the Avrami exponent is 3, and do not vary with the composition. However, for the composites, Avrami exponent varies with HDPE content in a rather complex manner. This can be attributed to the different nucleation mechanisms. The dramatic changes of melting and crystallization behaviors for the composites containing 30–35 wt % HDPE correspond to the sudden change in the morphology of the two phases, which is supported by the observation of SEM and electrical measurement. This suggests that crystallization investigation can also be used to characterize the morphology of polymer blends.

#### Acknowledgements

This work was supported by United Nations Educational, Scientific and Cultural Organization (UNESCO) and the Ministry of Education, Science and Culture of Japan (MONBUSHO). Authors want to thank Dr J. Z. Wang for his valuable discussion.

#### References

1. L. A. UTRACKI, *Polym. Eng. Sci.* **22** (1982) 1166.
2. J. K. CAO, J. Z. WANG, Y. CHEN and Z. W. WU, *J. Appl. Polym. Sci.* **59** (1996) 509.
3. R. FARYT, R. JEROME and Ph. TEYSSIE, *Polym. Eng. Sci.* **27** (1987) 328.
4. J. W. BARLOW and D. R. PAUL, *ibid.* **24** (1984) 525.
5. A. P. POLOCHOCKI, *ibid.* **26** (1986) 82.
6. K. MIN, J. L. WHITE and J. F. FELLERS, *ibid.* **24** (1984) 1327.
7. E. MARTUSCELLI, *Polym. Eng. Sci.* **24** (1984) 563.
8. O. O. SANTANA and A. J. MULLER, *Polym. Bull.* **32** (1994) 471.
9. A. SIEGMANN, *J. Appl. Polym. Sci.* **27** (1982) 1053.
10. R. GRECO, C. MANCARELLA, E. MARTUSCELLI, G. RAGOSTA and J. H. YIN, *Polymer* **28** (1987) 1929.
11. V. M. NADKARNI and J. P. JOG, *J. Appl. Polym. Sci.* **32** (1986) 5817.
12. E. MARTUSCELLI, M. PRACELLA, M. AVELLA, R. GRECO and G. RAGOSTA, *Makomol. Chem.* **25** (1980) 1703.

13. A. J. LOVINGER and M. L. WILLIAMS, *J. Appl. Polym. Sci.* **25** (1980) 1703.
14. A. LECLAIR and B. D. FAVIS, *Polymer* **37** (1996) 4723.
15. R. K. KRISHNASWAMY and D. S. KALIKA, *Polym. Eng. Sci.* **36** (1996) 786.
16. *Idem.*, *Polymer* **35** (1994) 1157.
17. D. S. KALIKA and R. K. KRISHNASWAMY, *Macromolecules* **26** (1993) 4252.
18. U. SUNDARARAJ and C. W. MACOSKO, *Polym. Eng. Sci.* **36** (1996) 1769.
19. E. MARTUSCELLI, C. SILVESTRE and L. BIANCHI, *Polymer* **24** (1983) 1458.
20. L. YU, R. A. SHANKS and Z. H. STACHURSKI, *J. Mater. Sci. Lett.* **15** (1995) 610.
21. Z. H. STACHURSKI, G. H. EDWARD, Y. MEI and L. YU, *Macromolecules*, **29** (1996) 2131.
22. G. D. WIGNALL, J. D. LONDONO, J. S. LIN, R. G. ALAMO, M. J. GALANTE and L. MANDELKERN, *ibid.* **28** (1995) 3156.
23. J. MINICK, A. MOET and E. BAER, *Polymer* **36** (1995) 1923.
24. A. GAIESKI, M. PRACELLA and E. MARTUSCELLI, *J. Polym. Sci., Polym. Phys. Edn.* **24** (1984) 739.
25. A. GAIESKI, Z. BARTCZAK and M. PRACELLA, *Polymer* **25** (1984) 1323.
26. A. K. GUPTA, V. B. GUPTA, R. H. PETERS, W. G. HARLAND and J. P. BERRI, *J. Appl. Polym. Sci.* **27** (1982) 4669.
27. J. M. KENNY and A. MAFFEZZOLI, *Polym. Eng. Sci.* **31** (1991) 607.
28. Y. LEE and R. S. PORTER, *ibid.* **26** (1986) 633.
29. G. P. DESIO and L. REBENFELD, *J. Appl. Polym. Sci.* **39** (1990) 825.
30. C. AUER, G. KALINKA, TH. KRAUSE and G. HINRICHSSEN, *ibid.* **51** (1994) 407.
31. N. A. MECHL and L. REBENFELD, *ibid.* **57** (1995) 187.
32. T. E. SUKHANOVA, F. LEDNICKY, J. URBAN, Y. G. BAKLAGINA, G. M. MIKHAILOV and V. V. KUDRYAVTSEV, *J. Mater. Sci.* **30** (1995) 2201.
33. S. NAGAE, Y. OTSUKA, M. NISHIDA, Y. SHIMIZU, T. TAKADA and S. YUMITORI, *J. Mater. Sci. Lett.* **14** (1995) 1234.
34. J. P. JOG and V. M. NADKARNI, *J. Appl. Polym. Sci.* **30** (1985) 997.
35. C. ZHANG, X. S. YI, H. YUI, S. ASAI and M. SUMITA, *Mat. Lett.* **36** (1998) 186.
36. C. ZHANG, X. S. YI, H. YUI, S. ASAI and M. SUMITA, *J. Appl. Polym. Sci.* **69** (1998) 1813.
37. B. D. FAVIS and J. P. CHALIFOUX, *Polymer* **29** (1988) 1761.
38. B. D. FAVIS and J. M. WILLIS, *J. Polym. Sci.* **28** (1990) 2259.
39. C. D. HAN, in "Multiphase flow in polymer processing" (Academic Press, New York, 1981).
40. A. LUCIANI and J. JARRIN, *Polym. Eng. Sci.* **36** (1996) 1619.
41. K. MIN, J. L. WHITE and J. F. FELLERS, *ibid.* **24** (1984) 1327.
42. M. SUMITA, K. SAKATA, S. ASAI, K. MIYASAKA and H. NAKAKAWA, *Polym. Bull.* **25** (1991) 265.
43. S. ASAI, K. SAKATA, M. SUMITA and K. MIYASAKA, *Polym. J.* **24** (1992) 415.
44. Z. BARTCZAK, A. GALESKI and M. PRACELLA, *Polymer* **27** (1986) 537.
45. F. GUBBELS, S. BLACHER, E. VANLATHEN, R. JEROME, R. DELTOUR, F. BROUERS and Ph. TEYSSIE, *Macromolecules* **28** (1995) 1559.
46. C. O. HAMMER and F. H. MAURTER, *Polymer Composites* **19** (1998) 116.
47. M. AVRAMI, *J. Chem. Phys.* **7** (1939) 1103; **8** (1940) 212; **9** (1941) 177.

Received 19 June 1998  
and accepted 22 July 1999